JOURNAL OF MATERIALS SCIENCE **39** (2004) 6583–6589

High temperature oxidation behavior of Ti-Al-Nb ternary alloys

YONG SHEN, XIAOFEI DING, FUGANG WANG
Department of Material Engineering, Dalian University of Technology, Dalian 116024, People's Republic of China

Y. TAN, J.-M. YANG
Department of Materials Science and Engineering, University of California, Los Angeles, CA 90095-1595, USA
E-mail: jyang@seas.ucla.edu

The oxidation behavior of four Ti-Al-Nb ternary alloys with different microstructures were investigated at 1000°C using interrupted oxidation test in air. Alloys with single-phase γ-TiAl, two-phase γ-TiAl + α_2-Ti_3Al, multi-phase γ-TiAl + α_2-Ti_3Al + Nb_2Al and two-phase α_2-Ti_3Al + Nb_2Al were prepared. The oxidation resistance of the Ti-Al-Nb ternary alloy at high temperature was found to be better than that of the binary Ti-Al alloy. Among the four Ti-Al-Nb ternary alloys, the $\gamma + \alpha_2$ two-phase alloy has the best oxidation resistance. The presence of Nb-enriched phase such as Nb_2Al and Nb_3Al decrease the oxidation resistance at elevated temperature presumably due to the formation of Nb_2O_5, which would accelerate the exfoliation of oxide.

1. Introduction

The TiAl intermetallic compound is an attractive material for high-temperature structural applications because of its low density, high melting point and high specific strength at elevated temperature [1–3]. However, application of the alloy is restricted by its inferior ductility and deformability at room temperature, and poor oxidation resistance at high temperature [3, 4]. Alloying and surface treatment could improve the high temperature oxidation resistance of the TiAl alloy [5–15]. Shida and Anada classified alloying elements for TiAl alloy into three types; that is favorable elements such as Nb, Mo, W, Si, C and B, neutral elements and harmful elements [5]. Nb has been considered to be the most effective alloying element to improve the oxidation resistance of TiAl [16–18]. Thus far, the effect of alloying on the oxidation resistance of single-phase TiAl alloy has been well documented [1, 5, 19]. It also has been reported that the oxidation rate for a duplex microstructure is higher than that for a lamellar microstructure by comparing the same composition with different microstructure [20–23]. However, very few studies had been conducted to investigate the effect of morphology and microstructure on the oxidation resistance of TiAl [24].

The aim of present study is to systematically examine the oxidation resistance of Ti-Al-Nb ternary alloys as a heat-resistant alloy. The alloys were designed to have single-phase, two-phase and multi-phase microstructures by adjusting the composition of Ti, Al and Nb in Nb-Ti-Al ternary system. The effect of alloy composition and microstructure on oxidation resistance at 1000°C in static air was studied.

2. Experimental procedures

2.1. Alloy preparation

According to Ti-Al-Nb ternary phase diagrams [25, 26], the composition of the alloys used in this study was chosen as Ti-47.5 at%Al-5 at%Nb, Ti-42.8 at%Al-14.2 at%Nb, Ti-40 at%Al-20 at%Nb and Ti-30 at%Al-40 at%Nb (hereafter designated as alloy 1, alloy 2, alloy 3 and alloy 4). The main purpose of the composition design was to prepare the Ti-Al-Nb ternary alloys with single-phase, two-phase and multi-phase microstructure. A binary TiAl alloy near stoichiometry composition was also prepared for comparison. High purity Ti (99.9% pure), Al (99.9% pure) and Nb (99.9% pure) were used as the raw materials. All alloys, each about 25 g, were prepared by arc-melting using a tungsten electrode under argon. All the ingots were homogenized at 1200°C for 5 h in vacuum and cooled down to room temperature in the furnace. Specimens with dimensions of 8.0 mm × 4.0 mm × 2.0 mm were machined from the ingot. The specimens were all polished with up to 600# SiC paper and cleaned with acetone and ethanol before the isothermal oxidation experiment.

2.2. Experimental procedures

The interrupted isothermal oxidation experiment was carried out at 1000°C in air. The specimens were laid obliquely in a quartz crucible to ensure that the six sides of the alloy had full contact with the air. Three specimens of each alloy were used for oxidation experiment in order to get the average mass change. The specimens were periodically removed from the furnace, air cooled, weighed, and returned to the furnace for

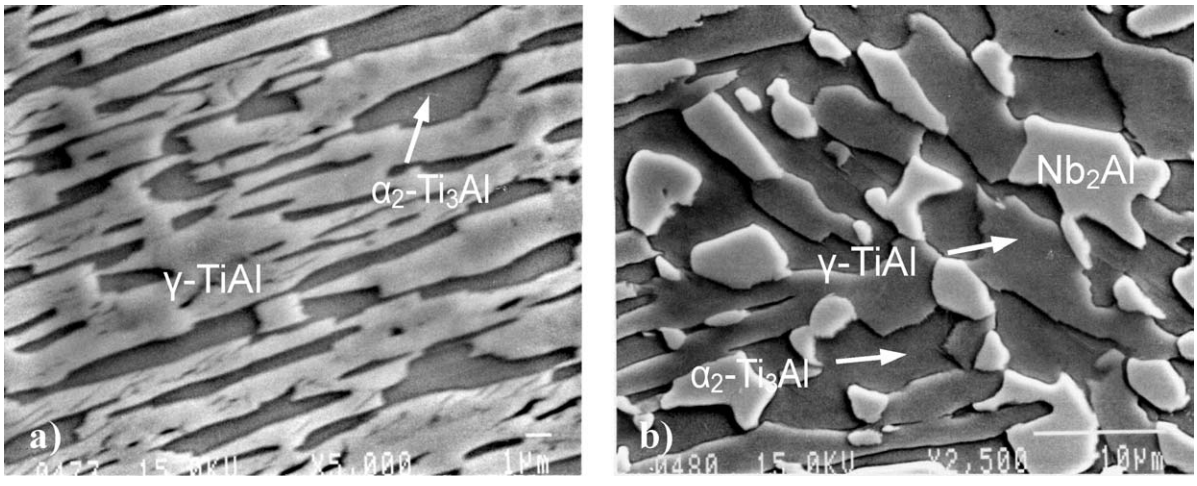

Figure 1 Micrographs of alloy 2 (a) and alloy 3 (b) after annealing at 1200°C for 5 h.

every 10 h. The total oxidation exposure was set to be 100 h. The mass gain was weighted by an electronic balance with accuracy at 0.1 mg. The microstructure of the specimen before and after the oxidation test were determined by X-ray diffraction (XRD) and microscopy. Scanning electron microscopy (SEM) equipped with an energy dispersive X-ray analysis system (EDS) was used to study the morphology of oxide scale. The elemental distribution across the oxide scale was analyzed by electron probe microanalysis (EPMA).

3. Results

3.1. Microstructures

Fig. 1 shows the representative micrographs of alloy 2 with lamellar structure and alloy 3 with mixed structure, respectively. Fig. 2 shows the XRD patterns of annealed alloy 1, 2 and 3, respectively. Based on microstructure observation and analyses of the results of XRD and EPMA, the microstructure of the four alloys annealed at 1200°C for 5 h were identified to be single-phase γ-TiAl for alloy 1, two-phase γ-TiAl + α_2-Ti_3Al for alloy 2, multi-phase γ-TiAl + α_2-Ti_3Al + Nb_2Al for alloy 3 and two-phase α_2-Ti_3Al + Nb_2Al for alloy 4, respectively. The phase contents of the microstructures of alloy 2, 3 and 4 are in agreement with the Nb-Ti-Al ternary phase diagram reported by Qu etc. [25], and that for alloy 1 is in agreement with Ding and Hao's paper [26]. We have referred to many Ti-Al-Nb ternary phase diagrams available in the literature. However, most of the Ti-Al-Nb ternary phase diagrams available are very different. The Ti-Al-Nb diagram needs further systematic investigation.

3.2. Oxidation kinetics

Fig. 3 shows the oxidation kinetic curves of the four alloys at tested 1000°C. The mass gains of the four alloys after interrupted oxidation test at 1000°C for 100 h were all less than 8 mg/cm^2. In particular, the $\gamma + \alpha_2$ two-phase alloy (alloy 2) showed the best oxidation resistance with a mass gain of only about 2.5 mg/cm^2. The mass gains of a binary TiAl alloy used in this study was found to be 69 mg/cm^2 at 1000°C for 100 h. The results suggest that the oxidation resistance of Ti-Al-Nb ternary alloys were superior to that of the Ti-Al binary alloys at 1000°C. Shida and Anada reported that the mass gains of Ti-Al binary alloys oxidized at 800°C for 100 h was about 1–3 mg/cm^2 [8, 27–30].

After oxidation test at 1000°C for 100 h, the outer layer of all specimens were all grayish-white. Also, some spalled-off oxide scales were found in the crucible. However, it should be noted that the time to spallation and the amount of spalled-off oxides for these four alloys were different. Alloy 2 had the least amount of spalled-off oxide scale, while alloy 4 had the most. The spallation of oxide scale occurred after oxidation at 1000°C for 30 h for alloy 1 and 4. The spallation did not occur for alloy 2 until after 90 h of oxidation test.

The variation of the oxidation mass gain with time shown in Fig. 3 could be expressed with Equation 1:

$$\Delta M^{\mathrm{n}} = k_{\mathrm{n}} t \tag{1}$$

where ΔM represents the oxide mass gain (mg/cm^2), n is the power exponent, k_{n} is the oxidation reaction rate constant (mg $\cdot$ cm^{-2} $\cdot$ h^{-1}), and t is the oxidation time (h). From Equation 1, the power exponent n and the oxidation reaction rate constant k_{n} could be determined by the fitted linear regression line of log (ΔM) on log (t). The results of each alloy are shown in Table I.

Based on the results listed in Table I, it appears that the rate constant of alloy 1, 3 and 4 was close to 1, and their kinetic curves followed the linear law. However, the rate constant of alloy 2 was higher than 2, and its curve followed the parabolic law. Combining the above kinetic results and observation, it could be concluded that during the oxidation process, alloy 1, 3 and 4 continued to oxidize due to their inability to form a stable protective oxide scale, while alloy 2 formed a protective oxide scale, inhibiting the oxidation to some extent.

TABLE I Kinetic parameters of interrupted oxidation of the alloy at 1000°C

	n	k_{n}
Alloy 1	1.3	0.076
Alloy 2	2.2	0.078
Alloy 3	1.0	0.052
Alloy 4	1.0	0.079

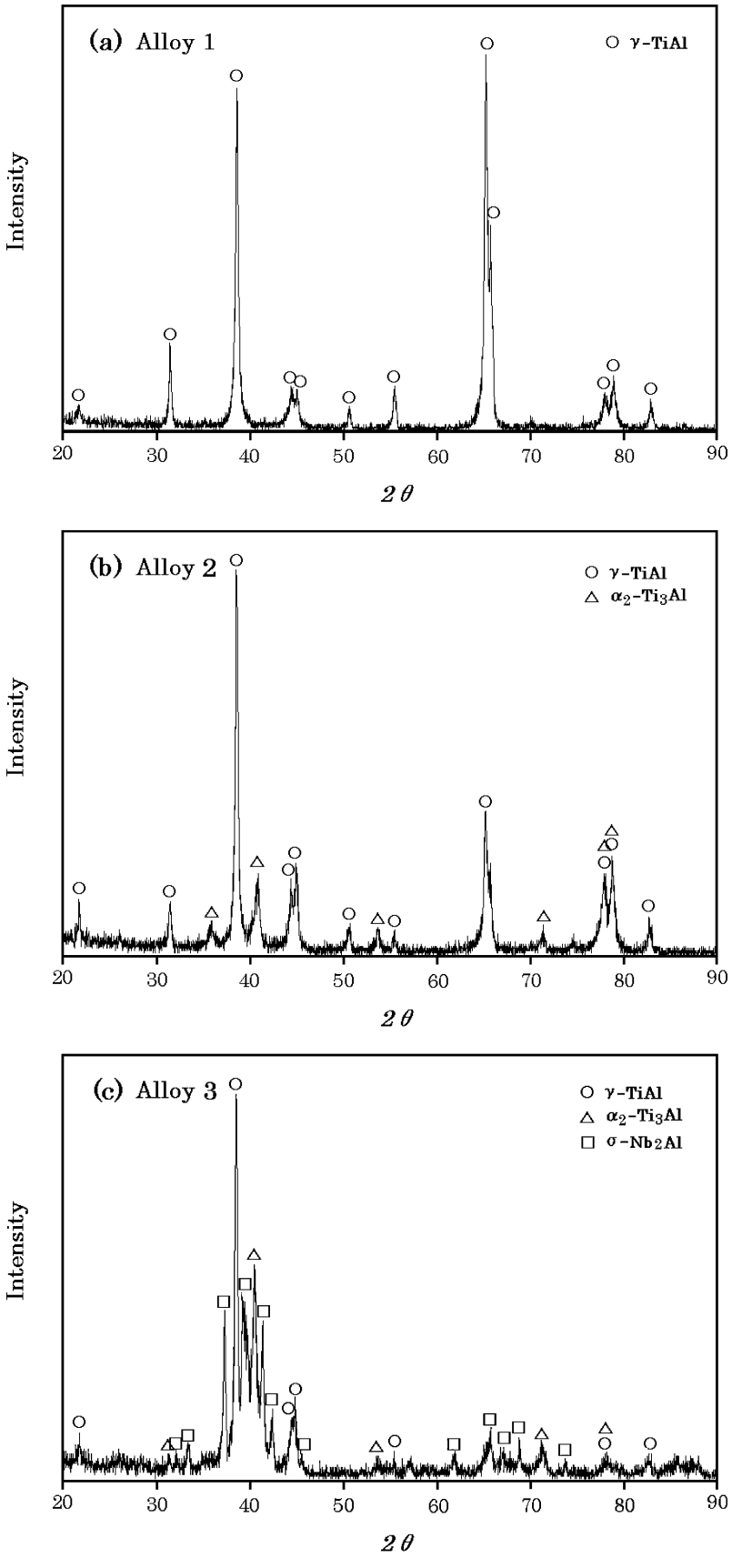

Figure 2 XRD profiles of alloy 1 (a), alloy 2 (b), and alloy 3 (c) after annealing at 1200°C for 5 h.

3.3. Microstructure and compositional analysis of oxide scale

The microstructure and composition across the oxide scale for these four alloys were analyzed using X-ray diffraction, SEM/EDS and EPMA. The results are summarized the following sections.

3.3.1. Ti-Al-Nb single-phase alloy

Fig. 4a shows the surface SEM micrograph of alloy 1 oxidized at 1000°C for 100 h. The surface morphology exhibited a nodular/granular structure. Fig. 5a shows the cross-section SEM micrograph of alloy 1. The thickness of oxide scale was found to be about 10 μm, and

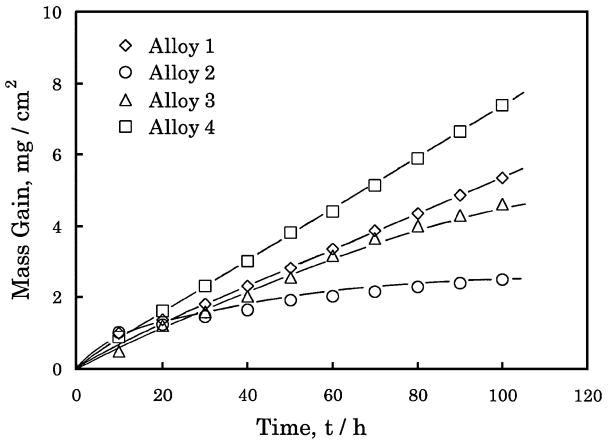

Figure 3 Kinetic curves of interrupted oxidation of Ti-Al-Nb ternary alloy at 1000°C.

it stratified into two layers: the external scale and the internal scale which was close to matrix. The EPMA spectra of alloy 1 across the oxide scale is shown in Fig. 6. It revealed that inner scale contained Ti, Al and Nb, where the concentration of Ti was relatively small.

According to these results of EDS, EPMA analysis and X-ray diffraction, it is evident that the inner scale was a mixed oxide of Al_2O_3 and TiO_2, and the outer scale was mainly composed of TiO_2.

3.3.2. Ti-Al-Nb two-phase and multi-phase alloys

The surface morphology of a two-phase $\gamma+\alpha_2$ alloy (alloy 2) after oxidation test at 1000°C for 100 h is shown in Fig. 4b. The nodule on the oxide scale was very fine. Fig. 5b shows the cross-section SEM micrograph of alloy 2. Both of EDS and EPMA analysis showed that the oxide scale contained little Ti and Nb. X-ray diffraction result as shown in Fig. 7a also indicated that the oxide scale primarily consisted of Al_2O_3 and a minor amount of TiO_2. Alloy 2 had the best oxidation resistance in this study, which may be due to the formation of a stable protective Al_2O_3 scale.

The surface morphology of a $\gamma+\alpha_2+Nb_2Al$ alloy (alloy 3) is shown in Fig. 4c. The oxide scale of alloy 3 was composed of a multi-layered scale and the thickness of about 20 μm as shown in Fig. 5c. EDS analysis and X-ray diffraction results as shown in Fig. 7b verified that the oxide scale is composed of a mixed oxide of Al_2O_3, TiO_2 and Nb_2O_5. The alloy exhibited apparent spallation of oxide scale from the substrate. The presence of Nb_2O_5 would promote the exfoliation of oxide scale.

The surface morphology of a two-phase α_2+Nb_2Al alloy (alloy 4) is shown in Fig. 4d. The nodule on the oxide scale was very coarse and porous. EDS analysis and X-ray diffraction also indicated the oxide scale was composed of Al_2O_3, TiO_2 and Nb_2O_5. Fig. 5d shows the cross-section SEM micrograph of alloy. The outer oxide scale also exfoliated completely.

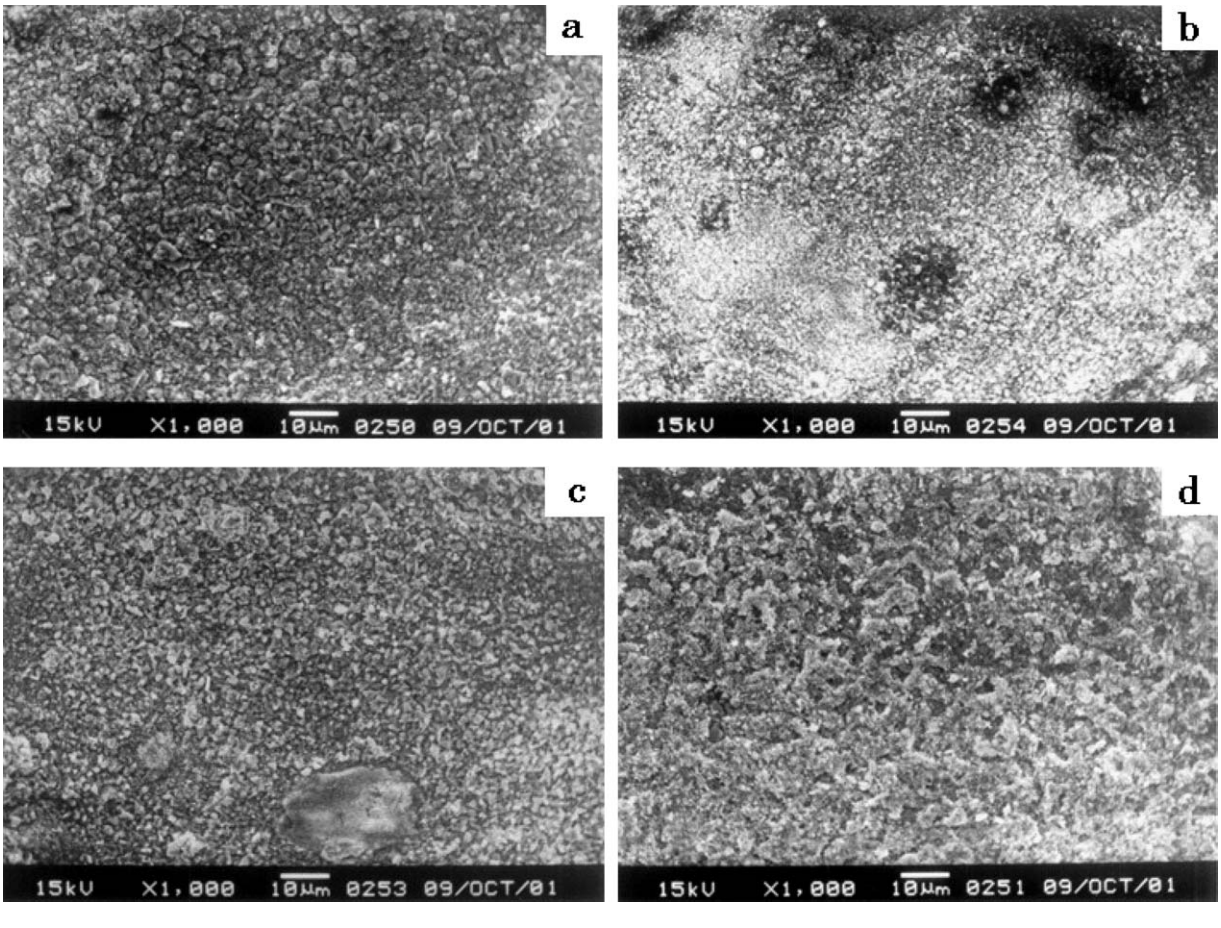

Figure 4 Surface SEM morphologies of the alloy oxidized at 1000°C for 100 h: (a) Alloy 1, (b) Alloy 2, (c) Alloy 3 and (d) Alloy 4.

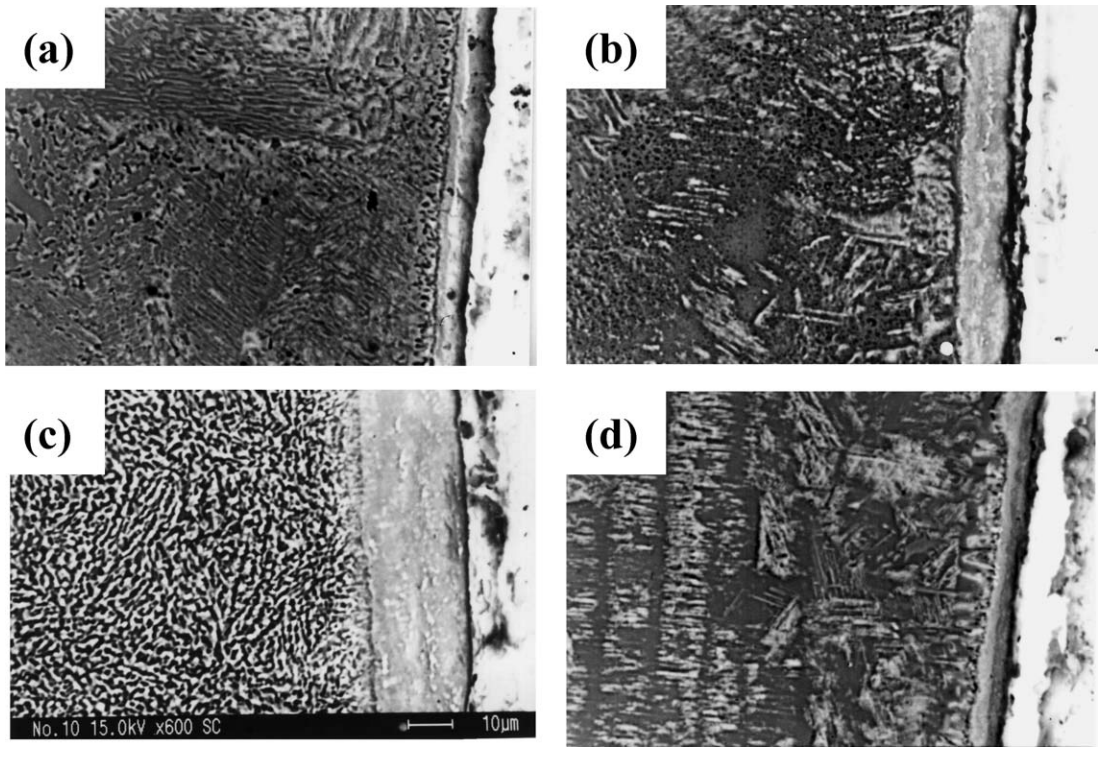

Figure 5 Cross-section micrograph of the alloys: (a) Alloy 1, (b) Alloy 2, (c) Alloy 3, and (d) Alloy 4.

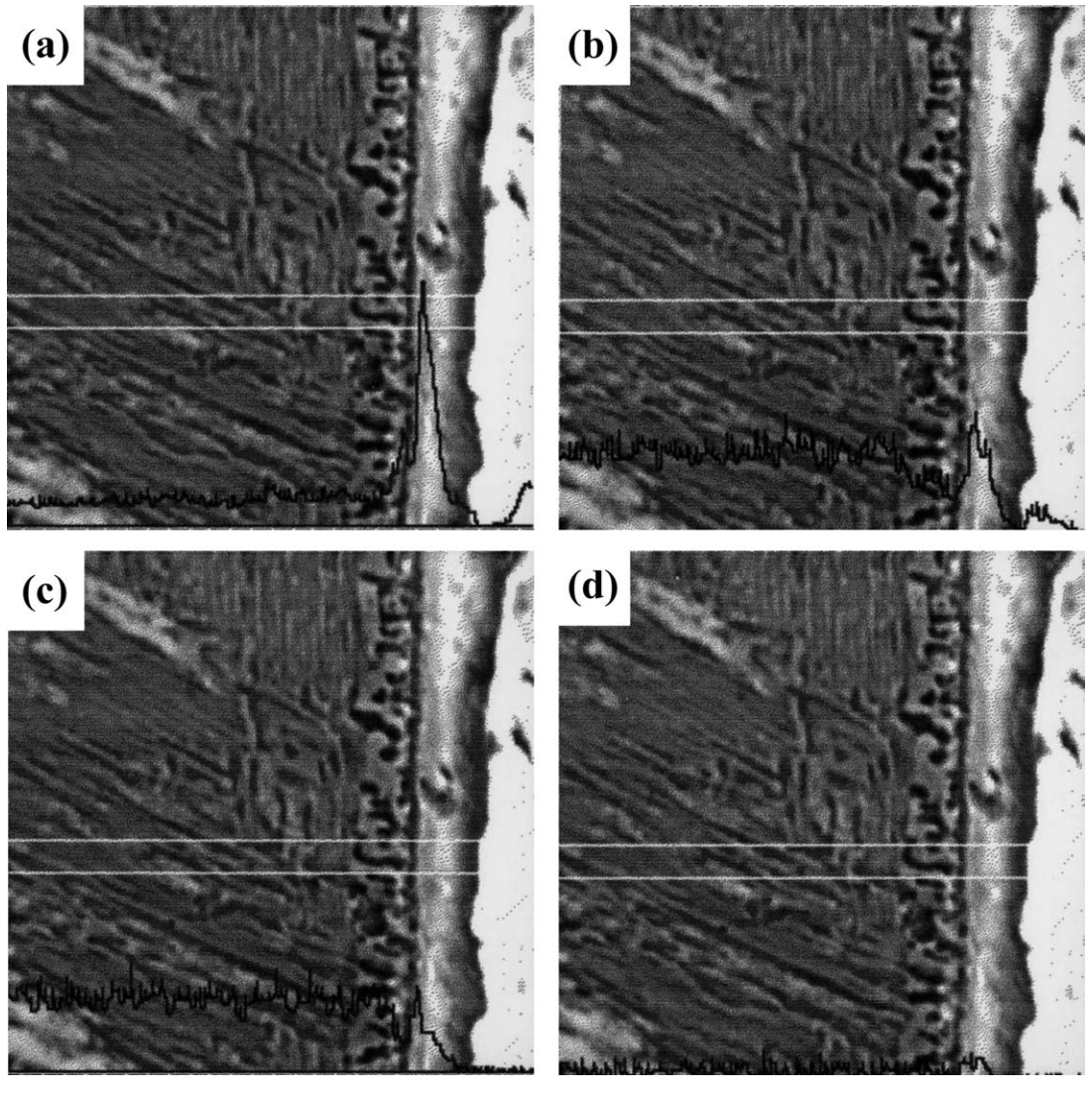

Figure 6 Cross-section micrograph and its EPMA spectra of alloy 1: (a) O profile, (b) Al, (c) Ti, and (d) Nb.

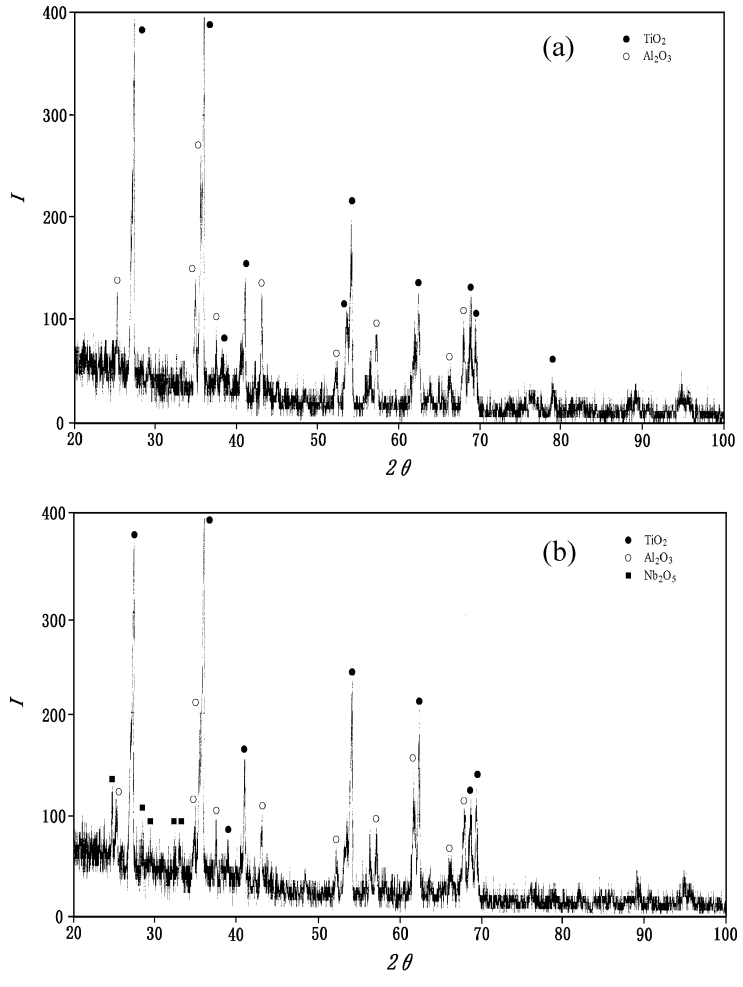

Figure 7 XRD profiles of the oxide scale of alloy 2 (a) and alloy 3 (b) after oxidized at 1000°C for 100 h.

4. Discussion

The above results clearly show that the oxidation behavior of Ti-Al-Nb alloys is superior to that of the binary Ti-Al alloy. In generally, the free energy of formation of TiO_2 and Al_2O_3 in Ti-Al binary system is very close. At the same time, the activity of Al shows negative deviation, so the selective oxidation of Al is difficult to take place at high temperature [6]. As a result, the alloy forms a mixed oxide of Al_2O_3 and TiO_2, rather than the protective oxide of Al_2O_3. The structure of TiO_2 is porous and, thus, is the fast diffusion channel of oxygen. At high temperature TiO_2 is less protective than Al_2O_3 even if the TiO_2 were not porous due to the higher concentration of point defects. Also the adhesion of the Al_2O_3 + TiO_2 mixed oxides to the substrate is poor, which result in poor oxidation resistance of the binary Ti-Al alloy. Adding a small amount of Nb in the alloy could increase the activity of Al, suppress the growth of TiO_2, promote the formation of protective oxide scale of Al_2O_3, and thus reduce the oxidation rate of the alloy. The addition of Mo or Sb to Ti-Al binary alloys has similar effect [14, 15].

The above results also show that the oxidation behavior of Ti-Al-Nb alloys is influenced by the microstructure and alloy composition. In the single-phase alloy (alloy 1), the non-protective oxide of TiO_2 dominated the outer oxide scale. Therefore, the formation of the inner oxide scale and the stability of Al_2O_3 in the inner oxide scale should control the oxidation rate. The $\gamma + \alpha_2$ two-phase alloy (alloy 2) has the best oxidation resistance in this study. According to several previous studies in Ti-Al binary alloys, the oxidation resistance improves with aluminum content, so the oxidation resistance of α_2 is generally inferior to that of γ [8, 27–30]. However, in this study of Ti-Al-Nb ternary system, the oxidation resistance of $\gamma + \alpha_2$ two-phase alloy was found to be better than γ single-phase alloy. The improvement of oxidation resistance may be attributed to the higher amount of Nb present in both γ and α_2 phases.

Table II shows the results of EPMA elemental analysis for both alloys 1 and 2 after annealing. The Nb concentration in alloy 1 was detected to be around 5.1 at%. In the alloy 2, the Nb in the γ and α_2 phases were found to be 13.3 at% and 19.4 at%, respectively. Nb has been considered to be the most effective element

TABLE II The results of EPMA analysis for alloy 1 and 2 after annealing (at%)

		Ti	Al	Nb
Alloy 1	γ phase	47.7	47.1	5.1
Alloy 2	γ phase	38.0	48.7	13.3
	α_2 phase	49.2	31.4	19.4

to improve the oxidation resistance of TiAl [16–18]. As a result, the oxidation resistance of γ-phase in alloy 2 is expected to be better than that of alloy 1 because of its higher Nb concentration. Similarly, oxidation resistance of the α_2 phase in Ti-Al-Nb ternary alloy should be better than that of α_2 phase in Ti-Al binary [16–18].

It is also obvious that the Nb_2O_5 emerged in both alloy 3 and alloy 4 when the Nb content in the Ti-Al-Nb alloy is over 20 at%, resulting in the spallation of oxide scale. The spallation of oxide scale of alloys 3 and 4 must be related to the Nb-enriched phase of Nb_2Al. The poor oxidation resistance of Nb-based alloy and Nb-containing intermetallics such as Nb_3Al and Nb_2Al are mainly attributed to the weak adhesion between matrix and Nb_2O_5 formed even at 900°C [31]. The results obtained from this study can be used for optimizing the alloy composition and microstructure of oxidation-resistant Ti-Al-Nb ternary alloy.

5. Conclusion

On the basis of the above investigation on the oxidation behavior of Ti-Al-Nb ternary alloys, the following conclusions were obtained:

(1) The oxidation resistance of the Ti-Al-Nb ternary alloy at high temperature is better than that of the Ti-Al binary alloy.

(2) Among the four Ti-Al-Nb ternary alloys investigated in this study, the two-phase $\gamma + \alpha_2$ alloy has the best oxidation resistance because higher Nb concentration in both phases.

(3) The presence of a Nb-enriched phase, such as Nb_2Al and Nb_3Al, appears to decrease the oxidation resistance at elevated temperature presumably due to formation of Nb_2O_5 which would promote the spallation of the oxide scale.

References

1. Y. G. ZHANG, Y. F. HAN, G. L. CHEN and J. T. GUO, "Structural Intermetallics" (National Defense Industry Press, Beijing, 2001).
2. D. L. LIN, *J. Shanghai Jiaotong Univ.* **32**(2) (1998) 95.
3. D. M. DIMIDUK, *Mater. Sci. Eng.* A **263**A (1999) 281.
4. Y. W. KIM, *JOM* **46**(7) (1994) 30.
5. Y. SHIDA and H. ANADA, *Mater. Trans. JIM* **35** (1994) 623.
6. HENG QIANG YE, *Mater. Sci. Eng.* A **263**A (1999) 289.
7. Y. Q. YAN, W. S. WANG, Z. Q. ZHANG, Q. HONG, G. Z. LUO and L. ZHOU, *Trans. Metal Heat Treatm.* **21**(3) (2000) 1.
8. H. ANADA and Y. SHIDA, *Mater. Trans. JIM* **36**(4) (1995) 533.
9. YAO-CAO ZHU, Y. ZHANG, X. Y. LI, K. FUJITA and N. IWAMOTO, *ibid.* **41**(9) (2000) 1118.
10. ZHAOLIN TANG, FUHUI WANG and WEITAO WU, *Mater. Sci. Eng.* A **276** (2000) 70.
11. CHUNGEN ZHOU, YING YANG, S. K. GONG and H. B. XU, *ibid.* **307** (2001) 182.
12. H. L. QU, L. ZHOU, H. R. WEI and Y. Q. ZHAO, *Chinese J. Rare Met.* **25**(2) (2001) 81.
13. W. WANG, J. Y. SHI, Y. G. ZHANG and T. H. CHANG, *J. Beijing Univ. Aeron. Astron.* **27**(2) (2001) 125.
14. Y. H. HE, B. Y. HUANG, X. H. QU, C. M. LEI and L. H. CHEN, *J. Aeron. Mater.* **15**(3) (1995) 19.
15. J. CHEN, B. Y. HUANG, Y. TAN, G. ZHANG and C. L. MA, *Mater. Sci. Techn.* (Chinese) **6**(4) (1998) 11.
16. K. MAKI, M. SHIODA and M. SAYASHI, *Mater. Sci. Eng.* A **153** (1992) 591.
17. V. A. C. HAANAPPEL, H. CLEMENS and M. F. STROOSNIJDER, *Intermetallics* **10** (2002) 293.
18. W. ZHANG, G. CHEN and Z. SUN, *Scr. Metall. Mater.* **28**(5) (1993) 563.
19. X. J. WANG, H. W. CHANG and M. K. LEI, *Acta Metallurgica Sinica* **37**(8) (2001) 813.
20. P. PÉREZ and P. ADEVA, in "Intermetallics and Superalloys, EUROMAT 99," edited by D.G. Morris, S. Naka and P. Caron, (Wiley-VCD Verlag GmbH, Weinheim, Germany, 2000) Vol. 10, p. 194.
21. A. GIL, E. WALLURA, H. GRÜBMEIER and W. J. QUADAKKERS, *J. Mater. Sci.* **28** (1993) 5869.
22. A. GIL, H. HOVEN, E. WALLURA and W. J. QUADAKKERS, *Corr. Sci.* **34** (1993) 615.
23. A. C. HAANAPPEL, R. HOFMAN, J. D. SUNDERKÖTTER, W. GLATZ, H. CLEMENS and M. F. STROOSNIJDER, *Oxid. Met.* **48**(3/4) (1997) 263.
24. L. H. CHEN, Y. H. HE, P. CAO, B. Y. HUANG and X. H. QU, *Hot Working Techn.* **6** (1995) 7.
25. H. L. QU, L. ZHOU and H. R. WEI, *Rare Metal Mater. Engng.* **29**(1) (2000) 8.
26. JIN-JUN DING and SHI-MING HAO, *Intermetallics* **6** (1998) 329.
27. H. ANADA and Y. SHIDA, *Oxid. Met.* **45**(1/2) (1996) 197.
28. *Idem.*, *Corr. Sci.* **35**(5–8) (1993) 945.
29. *Idem.*, *Mater. Trans. JIM* **34**(3) (1993) 263.
30. *Idem.*, *J. Jap. Inst. Met.* **36**(7) (1994) 745.
31. H. W. LAVENDEL and A. G. ELLIOT, *Trans. Metall. Soc. AIME* **239** (1967) 143.

Received 11 December 2002
and accepted 3 June 2004